Observer Backstepping Control for Variable Speed Wind Turbine

Roberto Galeazzi and Mikkel P. S. Gryning and Mogens Blanke

Abstract— **This paper presents an observer backstepping approach to the variable speed control of wind turbines for maximizing wind power capture when operating between cut-in and rated wind speeds. The wind turbine is modeled as a two-mass drive-train system controlled by generator torque. The nonlinear controller relies on output feedback backstepping to regulate the generator torque such that a constant tip-speed-ratio can be obtained. The rotor speed is fed back while torsion angle and generator speed are estimated using a linear observer based on the dynamics of the system. The proposed scheme shows smooth and asymptotic tracking of the rotor speed as illustrated by simulation results.**

I. INTRODUCTION

In order for wind energy to gain further attention by governments worldwide, the cost of the produced energy must match other competing sources, e.g. coal and gas power. The environmental awareness has only increased, and many countries are showing a large interest in deploying offshore wind power plants. Due to the high risk and capital investment needed to build offshore wind power, the energy produced is supported locally through various regulations, often subsidiaries. When the deployment of offshore wind parks reach an industrialized state, the subsidiaries will be out phased, but the maintenance cost will not be reduced. The challenging task of controlling wind turbines for maximum energy output while minimizing drive train stress is therefore of high interest.

The complexity of wind turbine models is a great challenge due to the many degrees of freedom needed to include the most important dynamic effects. The main focus in this article is controlling the drive-train as it is the part which has the most wear, and is a limiting factor in maximizing wind energy capture. The focus of wind turbine control is divided into two regions as a function of the wind speed as shown in Fig. 1. The goal in the region between cut-in and rated is to maximize energy capture. In case of wind speeds in the operational range between rated and cut-out, the goal is to keep a constant angular velocity to limit generated noise, stress and vibrations on mechanical and structural components while maintaining the maximum rated power generation. When the power is below rated value, the system should maintain its pitch angle at the optimal value and control the generator torque to achieve optimal tip-speed ratio(TSR) which is a function of the pitch angle. The pitch angle of the rotor blades determine the relative angle with respect to wind direction and thereby turbine speed, and is assumed kept constant such that the turbine speed solely is regulated indirectly by opposing the aerodynamic torque using generator torque control. Achieving optimal tip-speed ratio then simplifies to keeping the rotor blades spinning at a rotational frequency related to that of the incoming wind. The choice of operating at the optimal wind tip speed ratio is based on the turbulent wake a blade makes when passing through an air stream. Extracting power from turbulent wind is less efficient and will subject the blades to high vibration stress, i.e. the angular speed of the rotor must match the settling time of the wind for optimum power capture.

The modeling of drive-trains varies with regard to assumptions of stiffness in the shafts, damping, inertia assessment and efficiency. The drive-train used is modeled as a two-mass system which compared to the traditional one-mass model includes torsional effects. Further increasing model complexity adds an unnecessary level of detail, and there is a major consensus that a two-mass model is sufficient for representing the important dynamics in power system stability studies from which this study originates. The aerodynamic torque affecting the high-speed shaft is nonlinear, thus making the resulting system nonlinear and challenging to control in an optimum manner.

The control strategies proposed for variable speed wind turbines in literature includes adaptive back-stepping control [5], feedback linearization [4], non-linear control using exact model knowledge and one adaptive type [8]. The conservative nature of the industry and commercial aspect of wind turbines have limited the implementation of advanced non-linear control, and methods such as gain-scheduling for classical controllers [1] and bump-less transfer in between local robust controllers [6] have been favored. Wind turbines are time varying with respect to efficiency, mechanical and electrical systems, making LPV based control [7] and adaptive robust methods viable as they guarantee stability in a large range of model perturbations.

This paper proposes an observer backstepping controller for the variable speed wind turbine in order to maximize wind power capture. The output backstepping controller fully exploits the nonlinear two-mass drive-train model of the wind turbine through the combination of a globally exponentially stable (GES) observer for the estimate of the torsion angle and of the generator shaft speed, and a globally asymptotically stable (GAS) controller that guarantees asymptotic

R. Galeazzi is with DTU Electrical Engineering, Technical University of Denmark, 2800 Kgs. Lyngby, Denmark rg@elektro.dtu.dk

M. P. S. Gryning is with the SCADA Department, DONG Energy, 2820 Gentofte, Denmark, and with DTU Electrical Engineering, Technical University of Denmark, 2800 Kgs. Lyngby, Denmark migry@dongenergy.dk

M. Blanke is with DTU Electrical Engineering, Technical University of Denmark, 2800 Kgs. Lyngby, Denmark, and is also adjunct prof. at the AMOS Centre of Excellence at Norwegian University of Science and Technology, 7491 Trondheim, Norway mb@elektro.dtu.dk

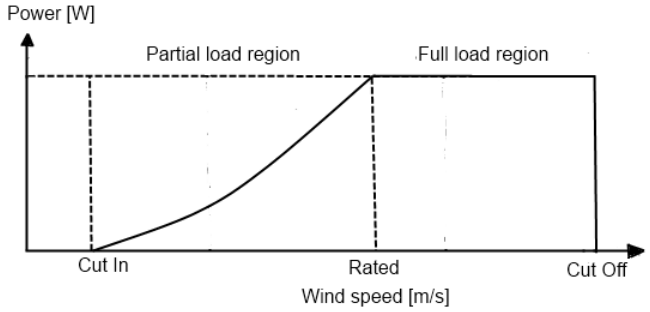

Fig. 1. Output power in different operating regions

tracking of the desired rotor speed and uniform ultimate boundedness (UUB) of the torsion angle.

II. MODEL

A. Wind power capture

The efficiency of a wind turbine is described using a power curve which is taken as a function of the pitch angle β and tip-speed-ratio λ. The power coefficient C_p is the ratio between aerodynamic rotor power P and the power available from the wind P_w, defining the ratio of power possible of capturing,

$$C_p = \frac{P}{P_w} \tag{1}$$

The power available is

$$P_w = \frac{1}{2}\rho A v^3 \tag{2}$$

where ρ is the air density, v is the wind speed and A is the swept area of the rotor which is given by πR_r^2, where R_r is the blade tip radius. From the definition of the power coefficient, the power captured by the wind turbine is,

$$P_m = \frac{1}{2}C_p(\lambda,\beta)\rho A v^3. \tag{3}$$

The tip-speed ratio λ is defined as

$$\lambda = \frac{R_r\omega}{v} \tag{4}$$

and it can be seen from (3) that operating at a fixed pitch angle makes the power coefficient C_p a function of only λ such that an optimal point on the power curve can be obtained by keeping λ constant. From the definition in (4) it is clear that λ is a function of the non controllable wind speed v, but also of the controllable rotor speed ω. In order to sustain maximum power output, the rotor speed must as a consequence be adjusted according to wind speed variation. The relationship between captured wind power, rotor speed and rotor torque is derived from (3) and (4) [8]

$$P(\omega) = k_w\omega^3 \tag{5}$$

$$T_a = \frac{P}{\omega} = k_w\omega^2 \tag{6}$$

where the constant k_w is given from the optimal value of C_p and λ

$$k_w = \frac{1}{2}C_p\rho\pi\frac{R_r^5}{\lambda^3}. \tag{7}$$

The rotor torque is applied to the low-speed shaft of the drive-train and the dynamics of the two-mass drive train system can now be set up.

B. Two-mass drive-train model

The two-mass drive-train model consists of two shafts interconnected by a gearbox. The aerodynamic torque drives the low-speed shaft at the rotor speed ω, while the gearbox increases the angular speed of the high speed shaft to w_g while lowering the torque. The drive-train thereby converts wind energy to mechanical energy and through the generator to electrical energy.

The inertia of the rotor and generator is respectively lumped into J_r and J_g, and T_{ls}, T_{hs} and T_g denote low speed shaft torque, high speed shaft torque and generator torque. The stiffness of the shafts are modeled through damping and torsional coefficients B_r,B_g, K_d and B_d. The inertia of the low speed shaft includes the inertia of the rotor, while the friction component includes bearing frictions. The dynamics of the low speed shaft is

$$J_r\dot{\omega} = T_a - T_{ls} - B_r\omega \tag{8}$$

while the high speed shaft has similar dynamics which includes the inertia of the gearbox and generator and adds the friction from bearing and gears,

$$J_g\dot{\omega_g} = T_{hs} - T_g - B_g\omega_g. \tag{9}$$

The drive train torsion is modeled by a torsion spring and a friction coefficient,

$$T_{ls} = K_d\theta_k + B_d\dot{\theta_k} \tag{10}$$

$$\theta_k = \theta_r - \theta_g/N_g \tag{11}$$

where N_g is the drive train gear ratio. The low speed and high speed shaft are interconnected by the gearbox such that

$$N_g = \frac{T_{ls}}{T_{hs}} = \frac{\omega_g}{\omega_{ls}}. \tag{12}$$

Combining equations (8) to (12) results in the following ODEs for the dynamics of the two-mass drive-train model

$$\dot{\theta}_k = \omega - \frac{1}{N_g}\omega_g \tag{13}$$

$$\dot{\omega} = \frac{1}{J_r}\left(-K_d\theta_k + k_w\omega^2 - (B_d + B_r)\,\omega + \frac{B_d}{N_g}\omega_g\right) \tag{14}$$

$$\dot{\omega}_g = \frac{1}{J_g}\left(\frac{K_d}{N_g}\theta_k + \frac{B_d}{N_g}\omega - \left(\frac{B_d}{N_g^2} + B_g\right)\omega_g - T_g\right) \tag{15}$$

III. OBSERVER BACKSTEPPING CONTROL

Given the third order nonlinear system (13)-(15) the control objective is to design a controller capable of dynamically varying the rotor angular velocity ω such that a desired speed reference can be tracked. This must be achieved assuming that the only available measurement is ω.

The strategy chosen is an output feedback controller based on the observer backstepping control [3]. First an observer is designed for the subsystem (θ_k, ω_g), which has an

exponentially stable estimation error dynamics. Then, a new system is considered where the unmeasured states dynamics is replaced with the observer dynamics. Hence backstepping is applied using the state estimates as virtual control inputs and considering the estimation errors as disturbances whose behavior must be dominated.

Since the control objective is reference tracking the system (13)-(15) is rewritten in terms of the tracking error $e_\omega \triangleq \omega - \omega_d$ where $\omega_d(t) \in \mathcal{C}^2$ is the bounded reference trajectory with bounded derivatives. By inserting e_ω into Eqs. (13)-(15) the following dynamics is obtained

$$\dot{\theta}_k = e_\omega + \omega_d - \frac{1}{N_g}\omega_g \tag{16}$$

$$\dot{e}_\omega = \frac{1}{J_r}\Bigg(- K_d\theta_k + k_w\left(e_\omega + \omega_d\right)^2 + \frac{B_d}{N_g}\omega_g - \left(B_d + B_r\right)\left(e_\omega + \omega_d\right)\Bigg) \tag{17}$$

$$\dot{\omega}_g = \frac{1}{J_g}\left(\frac{K_d}{N_g}\theta_k + \frac{B_d}{N_g}\left(e_\omega + \omega_d\right) - \left(\frac{B_d}{N_g^2} + B_g\right)\omega_g - T_g\right) \tag{18}$$

A. Observer Design

The observer is built as a copy of the (θ_k, ω_g) dynamics, that is

$$\dot{\hat{\theta}}_k = e_\omega + \omega_d - \frac{1}{N_g}\hat{\omega}_g \tag{19}$$

$$\dot{\hat{\omega}}_g = \frac{1}{J_g}\left(\frac{K_d}{N_g}\hat{\theta}_k + \frac{B_d}{N_g}\left(e_\omega + \omega_d\right) - \left(\frac{B_d}{N_g^2} + B_g\right)\hat{\omega}_g - T_g\right). \tag{20}$$

The estimation error dynamics is hence given by the following linear system

$$\dot{\mathbf{e}}_o = \mathbf{A}\mathbf{e}_o = \begin{bmatrix} 0 & -\frac{1}{N_g} \\ \frac{K_d}{J_g N_g} & -\frac{1}{J_g}\left(\frac{B_d}{N_g^2} + B_g\right) \end{bmatrix}\mathbf{e}_o \tag{21}$$

where $\mathbf{e}_0 = \left[\tilde{\theta}_k, \tilde{\omega}_g\right]^{\mathrm{T}}$. Due to linearity, exponential stability of the estimation error can be easily assessed by checking if the matrix $\mathbf{A}$ is Hurwitz; however the Lyapunov based analysis is here preferred.

Proposition 1: The origin of the estimation error dynamics (21) is GES.

Proof: Consider the Lyapunov function candidate

$$V_o(\mathbf{e}_o) = \mathbf{e}_o^{\mathrm{T}}\mathbf{P}_o\mathbf{e}_o \tag{22}$$

where

$$\mathbf{P} = \begin{bmatrix} \frac{N_g^2 B_g + B_d}{2K_d\beta_1} + \frac{\beta_1 K_d + \beta_2 J_g}{2\beta_1\beta_2\left(B_g + \frac{B_d}{N_g^2}\right)} & -\frac{J_g N_g}{2\beta_1 K_d} \\ -\frac{J_g N_g}{2\beta_1 K_d} & \frac{\beta_2 J_g^2 + \beta_1 J_g K_d}{2\beta_1\beta_2 K_d\left(B_g + \frac{B_d}{N_g^2}\right)} \end{bmatrix},$$

$\mathbf{P}_o = \mathbf{P}_o^{\mathrm{T}} > 0$, is the solution of the Lyapunov equation $\mathbf{P_o M} + \mathbf{M}^{\mathrm{T}}\mathbf{P_o} = -\mathbf{Q}$, with $\mathbf{Q} = \mathrm{diag}\{1/\beta_1, 1/\beta_2\}$ and $\beta_i > 0$. The derivative along the trajectories of (21) results in

$$\begin{aligned}\dot{V}_o(\mathbf{e}_o) &= \mathbf{e}_o^{\mathrm{T}}\left(\mathbf{P_o A} + \mathbf{A}^{\mathrm{T}}\mathbf{P_o}\right)\mathbf{e}_o \\ &= -\mathbf{e}_o^{\mathrm{T}}\mathbf{Q}\mathbf{e}_o \\ &\leq -\lambda_{\min}(\mathbf{Q})\left\|\mathbf{e}_o\right\|_2^2\end{aligned} \tag{23}$$

Hence the origin $\mathbf{e}_o = (0,0)^{\mathrm{T}}$ is GES [2, Theorem 4.10], and the estimation error is always bounded

$$\left\|\mathbf{e}_o(t)\right\| \leq \kappa_e\left\|\mathbf{e}_o(t_0)\right\| e^{\lambda_{\max}(\mathbf{M})(t-t_0)}, \quad \forall\, t \geq t_0 \tag{24}$$

where $\kappa_e > 0$ and $\Re\{\lambda_{\max}(\mathbf{M})\} < 0$. ■

Remark 2: It is worth noting that if a faster observer dynamics is needed then a standard reduced order observer could be used instead

$$\hat{\mathbf{x}}_2 = \mathbf{w} + \mathbf{L}y \tag{25}$$

$$\dot{\mathbf{w}} = \mathbf{M}\mathbf{w} + \mathbf{N}T_g + \mathbf{R}y \tag{26}$$

where $\hat{\mathbf{x}}_2 = [\hat{\theta}_k, \hat{\omega}_g]^{\mathrm{T}}$, $y = x_1 = \omega$ is the measured output, the matrices $\mathbf{M}$, $\mathbf{N}$, and $\mathbf{R}$ are design parameters, and $\mathbf{L}$ is the observer gain matrix.

B. Output Feedback Backstepping Controller

An output feedback backstepping controller is now designed for the system

$$\dot{e}_\omega = \frac{1}{J_r}\Bigg[- K_d\left(\hat{\theta}_k + \tilde{\theta}_k\right) + k_w\left(e_\omega + \omega_d\right)^2 - \left(B_d + B_r\right)\left(e_\omega + \omega_d\right) + \frac{B_d}{N_g}\left(\hat{\omega}_g + \tilde{\omega}_g\right)\Bigg] - \dot{\omega}_d \tag{27}$$

$$\dot{\hat{\omega}}_g = \frac{1}{J_g}\left[\frac{K_d}{N_g}\hat{\theta}_k + \frac{B_d}{N_g}\left(e_\omega + \omega_d\right) - \left(\frac{B_d}{N_g^2} + B_g\right)\hat{\omega}_g - T_g\right] \tag{28}$$

where the estimate $\hat{\omega}_g$ is used as virtual control to stabilize (27), and T_g is the physical control input.

Proposition 3: Consider the system (27)-(28), and the reference vector $\mathbf{\Omega}_d = [\omega_d(t), \dot{\omega}_d(t), \ddot{\omega}_d(t)]^{\mathrm{T}}$. The output feedback backstepping control law

$$T_g = T_g\left(\hat{\theta}_k, e_\omega, z, \mathbf{\Omega}_d\right)$$

with

$$\beta_1 > 0 \tag{29}$$

$$\beta_2 > 0 \tag{30}$$

$$\beta_3 > \frac{4k_w^2 N_g^2 K_d^2 + N_g^2 K_d^2\left(\frac{B_d^3}{N_g^3}\beta_1 + K_d^2\beta_2\right)^2}{4J_r^2 B_d^2} \tag{31}$$

$$\beta_4 > \frac{4k_w^2 + \left(\frac{B_d^3}{N_g^3}\beta_1 + K_d^2\beta_2\right)^2}{4J_r^2} \tag{32}$$

$$
\begin{aligned}
T_g\left(\hat{\theta}_k, e_\omega, z, \mathbf{\Omega}\right) \triangleq\ & J_g\left(\frac{K_d}{J_g N_g}-\frac{N_g K_d\left(\frac{B_d^3}{N_g^3}\beta_1+K_d^2\beta_2\right)}{J_r B_d}-\frac{2k_w N_g K_d}{J_r B_d}\left(e_\omega+\omega_d\right)\right)\hat{\theta}_k \\
& + J_g\left(\frac{B_d}{J_g N_g}-\frac{N_g K_d}{B_d}-\frac{N_g\left(\frac{B_d^3}{N_g^3}\beta_1+K_d^2\beta_2\right)\left(B_d+B_r\right)}{J_r B_d}\right)\left(e_\omega+\omega_d\right) \\
& + J_g\left(\frac{K_d}{B_d}+\frac{2k_w}{J_r}\left(e_\omega+\omega_d\right)\frac{\left(\frac{B_d^3}{N_g^3}\beta_1+K_d^2\beta_2\right)}{J_r}\right) z \\
& + J_g\left(\frac{K_d}{B_d}-\frac{1}{J_g}\left(\frac{B_d}{N_g^2}+B_g\right)+\frac{\left(\frac{B_d^3}{N_g^3}\beta_1+K_d^2\beta_2\right)}{J_r}+\frac{2k_w}{J_r}\left(e_\omega+\omega_d\right)\right)\alpha\left(\hat{\theta}_k, e_\omega, \mathbf{\Omega}_d\right) \\
& + J_g\left(\frac{2k_w^2 N_g}{J_r B_d}\left(e_\omega+\omega_d\right)^3-\frac{k_w N_g}{J_r B_d}\left(2\left(B_d+B_r\right)-\left(\frac{B_d^3}{N_g^3}\beta_1+K_d^2\beta_2\right)\right)\left(e_\omega+\omega_d\right)^2\right) \\
& + J_g\left(-\frac{N_g}{B_d}\left(\frac{B_d^3}{N_g^3}\beta_1+K_d^2\beta_2+B_d+B_r\right)\dot{\omega}_d+\frac{N_g J_r}{B_d}\ddot{\omega}_d\right) z \\
& + J_g\left(\beta_3+\beta_4\right)\left(1+\left(e_\omega+\omega_d\right)^2\right) z
\end{aligned} \tag{31}
$$

$$
\alpha\left(\hat{\theta}_k, e_\omega, \mathbf{\Omega}_d\right) \triangleq \frac{N_g}{B_d}\left(-k_w\left(e_\omega+\omega_d\right)^2+\left(B_d+B_r\right)\omega_d+K_d\hat{\theta}_k+J_r\dot{\omega}_d-\left(\frac{B_d^3}{N_g^3}\beta_1+K_d^2\beta_2\right)e_\omega\right) \tag{32}
$$

renders GAS the origin of the $(e_\omega, z, \mathbf{e}_o)$ system, where $T_g\left(\hat{\theta}_k, e_\omega, z, \mathbf{\Omega}_d\right)$ is shown in (31),

$$
z \triangleq \hat{\omega}_g - \alpha\left(\hat{\theta}_k, e_\omega, \mathbf{\Omega}_d\right) \tag{35}
$$

and $\alpha\left(\hat{\theta}_k, e_\omega, \mathbf{\Omega}_d\right)$ is shown in (32).

Proof: The first step is to stabilize the tracking error dynamics (27) through the virtual control $\hat{\omega}_g$. Consider the control Lyapunov function (CLF) candidate

$$
V_1\left(e_\omega, \mathbf{e}_o\right) = \frac{J_r}{2}e_\omega^2 + V_o\left(\mathbf{e}_o\right) \tag{36}
$$

whose derivative along the trajectories is given by

$$
\begin{aligned}
\dot{V}_1 = e_\omega\Bigg(& -K_d\left(\hat{\theta}_k+\tilde{\theta}_k\right)-\left(B_d+B_r\right)\left(e_\omega+\omega_d\right) \\
& + k_w\left(e_\omega+\omega_d\right)^2+\frac{B_d}{N_g}\left(\hat{\omega}_g+\tilde{\omega}_g\right)-J_r\dot{\omega}_d\Bigg) \\
& -\frac{1}{\beta_1}\tilde{\theta}_k^2-\frac{1}{\beta_2}\tilde{\omega}_g^2.
\end{aligned} \tag{37}
$$

The virtual control $\hat{\omega}_g = \alpha\left(\hat{\theta}_k, e_\omega, \mathbf{\Omega}_d\right)$ renders GAS the origin of the $(e_\omega, \mathbf{e}_o)$ system. In fact by inserting (32) into (37) $\dot{V}_1\left(e_\omega, \mathbf{e}_o\right)$ reads

$$
\begin{aligned}
\dot{V}_1 = & -\left(B_d+B_r\right)e_\omega^2 - K_d e_\omega\tilde{\theta}_k + \frac{B_d}{N_g}e_\omega\tilde{\omega}_g \\
& -\left(\frac{B_d^2}{N_g^2}\beta_1+K_d^2\beta_2\right)e_\omega^2-\frac{1}{\beta_1}\tilde{\theta}_k^2-\frac{1}{\beta_2}\tilde{\omega}_g^2 \\
\leq & -\left(B_d+B_r\right)e_\omega^2-\beta_1\left(\frac{B_d}{N_g}\left|e_\omega\right|-\frac{1}{2\beta_1}\left|\tilde{\omega}_g\right|\right)^2 \\
& -\beta_2\left(K_d\left|e_\omega\right|-\frac{1}{2\beta_2}\left|\tilde{\theta}_k\right|\right)^2-\kappa_1\left\|\mathbf{e}_o\right\|_2^2
\end{aligned} \tag{38}
$$

which is negative definite for (β_1, β_2) as in (29)-(30), and where $\kappa_1 = \max\left\{-\frac{3}{4\beta_1}, -\frac{3}{4\beta_2}\right\}$.

Introducing the error variable z as in (35) the design of the real control input T_g is undertaken. The z-dynamics reads

$$
\dot{z} = \dot{\hat{\omega}}_g - \frac{\partial\alpha}{\partial\hat{\theta}_k}\dot{\hat{\theta}}_k - \frac{\partial\alpha}{\partial e_\omega}\dot{e}_\omega - \frac{\partial\alpha}{\partial\mathbf{\Omega}_d}\dot{\mathbf{\Omega}}_d \tag{39}
$$

and the detailed expression can be found in Appendix A. Then consider the following CLF

$$
V_2\left(z, e_\omega, \mathbf{e}_o\right) = V_1\left(e_\omega, \mathbf{e}_o\right) + \frac{1}{2}z^2 + V_o\left(\mathbf{e}_o\right) \tag{40}
$$

whose derivative along the trajectories reads as

$$
\begin{aligned}
\dot{V}_2 \leq & -\left(B_d+B_r\right)e_\omega^2-\beta_1\left(\frac{B_d}{N_g}\left|e_\omega\right|-\frac{1}{2\beta_1}\left|\tilde{\omega}_g\right|\right)^2 \\
& -\beta_2\left(K_d\left|e_\omega\right|-\frac{1}{2\beta_2}\left|\tilde{\theta}_k\right|\right)^2-\kappa_1\left\|\mathbf{e}_o\right\|_2^2 \\
& -\frac{1}{\beta_3}\tilde{\omega}_g^2-\frac{1}{\beta_4}\tilde{\theta}_k^2+z\dot{z}
\end{aligned} \tag{41}
$$

The control input $T_g = T_g\left(\hat{\theta}_k, e_\omega, z, \mathbf{\Omega}\right)$ renders GAS the origin of the $(e_\omega, z, \mathbf{e}_o)$ system; in fact by inserting (31) into (41) $\dot{V}_2\left(z, e_\omega, \mathbf{e}_o\right)$ reads

$$\begin{aligned}\dot{V}_2 \leq \dot{V}_1 &- \frac{1}{J_g}\left(\frac{B_d}{N_g^2} + B_g\right) z^2 \\ &- \beta_3\left(\left|\left(e_\omega + \omega_d\right) z\right| - \frac{k_w N_g K_d}{J_r B_d \beta_3}\left|\tilde{\theta}_k\right|\right)^2 \\ &- \beta_3\left(|z| - \frac{N_g K_d\left(\frac{B_d^3}{N_g^3}\beta_1 + K_d^2\beta_2\right)}{2J_r B_d \beta_3}\left|\tilde{\theta}_k\right|\right)^2 \\ &- \beta_4\left(\left|\left(e_\omega + \omega_d\right) z\right| - \frac{k_w}{J_r\beta_4}\left|\tilde{\omega}_g\right|\right)^2 \\ &- \beta_4\left(|z| - \frac{\frac{B_d^3}{N_g^3}\beta_1 + K_d^2\beta_2}{2J_r\beta_4}\left|\tilde{\omega}_g\right|\right)^2 \\ &- \left(1 - \frac{k_w^2 N_g^2 K_d^2}{J_r^2 B_d^2 \beta_3} - \frac{N_g^2 K_d^2\left(\frac{B_d^3}{N_g^3}\beta_1 + K_d^2\beta_2\right)^2}{4J_r^2 B_d^2 \beta_3}\right)\tilde{\theta}_k^2 \\ &- \left(1 - \frac{k_w^2}{J_r^2\beta_4} - \frac{\left(\frac{B_d^3}{N_g^3}\beta_1 + K_d^2\beta_2\right)^2}{4J_r^2\beta_4}\right)\tilde{\omega}_g^2 \end{aligned} \tag{42}$$

■

which is negative definite for (β_3, β_4) as in (31)-(32).

C. Boundedness of the θ_k Dynamics

As last step in the design of the output tracking controller it is important to prove that the dynamics of the torsion angle θ_k remains bounded. Towards this end consider the candidate Lyapunov function

$$V_3\left(\theta_k\right) = \frac{1}{2}\theta_k^2 \tag{43}$$

whose derivative along the trajectory of (13) is

$$\begin{aligned}\dot{V}_3 &= \theta_k\Big[e_\omega + \omega_d - \frac{1}{B_d}\big(-k_w\left(e_\omega + \omega_d\right)^2 \\ &\quad + \left(B_d + B_r\right)\omega_d + K_d\left(\theta_k + \tilde{\theta}_k\right) \\ &\quad + J_r\dot{\omega}_d - \left(\beta_1 + \beta_2\right)e_\omega\big)\Big] \end{aligned} \tag{44}$$

$$\begin{aligned}&\leq -\frac{K_d}{B_d}\theta_k^2 + \left|\left(e_\omega + \omega_d\right)\right|\left|\theta_k\right| + \frac{k_w}{B_d}\left(e_\omega + \omega_d\right)^2\left|\theta_k\right| \\ &\quad + \frac{B_d + B_r}{B_d}\left|\omega_d\right|\left|\theta_k\right| + \frac{K_d}{B_d}\left|\tilde{\theta}_k\right|\left|\theta_k\right| \\ &\quad + \frac{J_r}{B_d}\left|\dot{\omega}_d\right|\left|\theta_k\right| + \frac{\beta_1 + \beta_2}{B_d}\left|e_\omega\right|\left|\theta_k\right|. \end{aligned} \tag{45}$$

The desired trajectory $\omega_d\left(t\right)$ is a class $\mathcal{C}^2$ bounded function with bounded first derivative, that is

$$\left|\omega_d\left(t\right)\right| \leq \omega_{d,\max} < \infty \tag{46}$$

$$\left|\dot{\omega}_d\left(t\right)\right| \leq \dot{\omega}_{d,\max} < \infty \tag{47}$$

Moreover the dynamics of the tracking error $e_\omega\left(t\right)$ was shown to be asymptotically stable hence

$$\left|e_\omega\left(t\right)\right| \leq \gamma\left(\left|e_\omega\left(t_0\right)\right|, t - t_0\right), \quad \forall t \geq t_0 \tag{48}$$

where $\gamma\left(r, s\right)$ is a class $\mathcal{KL}$ function; whereas the dynamics of the estimation error $\mathbf{e}_{\text{obs}}$ was shown to be exponentially stable therefore

$$\left|\tilde{\theta}_k\left(t\right)\right| \leq k_e\left|\tilde{\theta}_k\left(t_0\right)\right| e^{\lambda_{\max}(\mathbf{A})(t - t_0)}, \quad \forall t \geq t_0. \tag{49}$$

By replacing these upper bounds into (45) we obtain

$$\begin{aligned}\dot{V}_3 \leq &-\left(1 - \delta\right)\frac{K_d}{B_d}\theta_k^2 - \delta\frac{K_d}{B_d}\theta_k^2 \\ &+ \Bigg(\left(1 + \frac{\beta_1 + \beta_2}{B_d}\right)\gamma\left(\left|e_\omega\left(t_0\right)\right|, 0\right) \\ &+ \left(1 + \frac{B_d + B_r}{B_d}\right)\omega_{d,\max}\Bigg)\left|\theta_k\right| \\ &+ \Bigg(\frac{k_w}{B_d}\left(\gamma\left(\left|e_\omega\left(t_0\right)\right|, 0\right) + \omega_{d,\max}\right)^2 \\ &+ \frac{K_d}{B_d}k_e\left|\tilde{\theta}_k\left(t_0\right)\right| + \frac{J_r}{B_d}\dot{\omega}_{d,\max}\Bigg)\left|\theta_k\right| \\ \leq &-\left(1 - \delta\right)\frac{K_d}{B_d}\theta_k^2 \end{aligned} \tag{50}$$

for all $|\theta_k| > \mu$

$$\begin{aligned}\mu = \frac{B_d}{\delta K_d}\Bigg(&\left(1 + \frac{\beta_1 + \beta_2}{B_d}\right)\gamma\left(\left|e_\omega\left(t_0\right)\right|, 0\right) \\ &+ \left(1 + \frac{B_d + B_r}{B_d}\right)\omega_{d,\max} \\ &+ \frac{k_w}{B_d}\left(\gamma\left(\left|e_\omega\left(t_0\right)\right|, 0\right) + \omega_{d,\max}\right)^2 \\ &+ \frac{K_d}{B_d}k_e\left|\tilde{\theta}_k\left(t_0\right)\right| + \frac{J_r}{B_d}\dot{\omega}_{d,\max}\Bigg) \end{aligned} \tag{51}$$

whit $0 < \delta < 1$. Hence $\theta_k\left(t\right)$ is globally uniformly ultimately bounded.

IV. CONTROL STRATEGY TESTING

A. Operating point

The system is designed to operate in the partial load region, i.e the the interval of wind speeds ranging $5m/s$ to $12.3m/s$ for this particular wind turbine. A wind-speed ($\bar{v}$) and a tip-speed ratio ($\bar{\lambda}$) is selected and the state of the system is calculated. Using (4) the angular velocity of the rotor can be calculated and through (12) the angular velocity of the generator shaft ω_g can be found. Inserting (4) into (6) yields

$$\bar{T_a} = \frac{1}{2\bar{\omega}}\rho A\bar{v}^3 C_p(\bar{\lambda}, \bar{\beta}) \tag{52}$$

and utilizing (12) gives

$$\bar{T_g} = \frac{1}{N_g}\bar{T_a}. \tag{53}$$

TABLE I

SIMULATION PARAMETERS

$\bar{v}[m/s]$	$\bar{\lambda}$	$\bar{\beta}[^\circ]$	$T_a[MNm]$
10.33	8.00	0.00	2.17
$T_g[kNm]$	$\theta_k[m^\circ]$	$C_p(\lambda,\beta)$	
22.86	80.42	0.46	

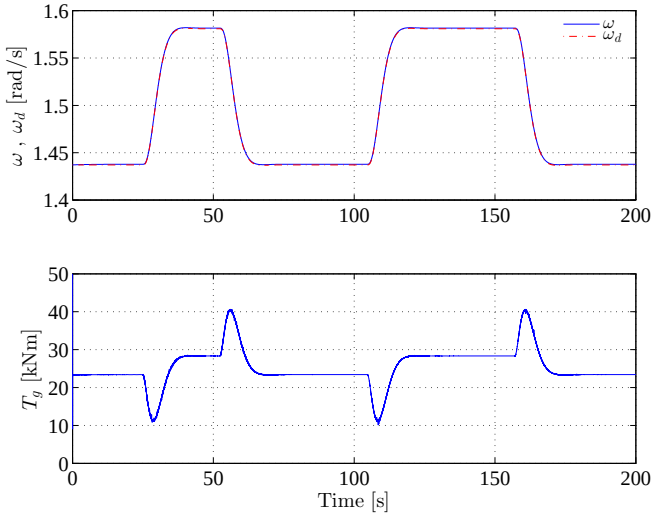

Fig. 2. Rotor speed tracking

The steady state torsion angle $\bar{\theta_k}$ can be found by inserting (10) into (8) which gives the following

$$\bar{\theta_k} = \frac{\bar{T_a} - B_r\bar{\omega}}{K_d}. \tag{54}$$

Equations (52)-(54) enables the non-linear simulation model to be initiated in an operating point. The tip-speed-ratio value selected for simulations reflects an initial condition of being in an position for maximum power generation. The values used in simulation are shown in Table I.

B. Testing

The rotor speed tracking of a square wave with a frequency of 0.06 radians per second and an amplitude of 10 percent of the operation point is shown in Fig. 2. It is clear that the proposed control scheme achieves smooth and precise asymptotic speed tracking.

V. CONCLUSIONS

Maximizing wind power capture in wind turbines is a major challenge given the constant evolution of the technologies involved and measurements available. In this work an output feedback backstepping approach has been proposed for the variable speed control of the wind turbine. Due to the challenges in measuring the torsion angle and generator speed a linear observer was designed and the estimation error dynamics was shown to be globally exponentially stable. Then an output feedback backstepping controller was designed exploiting the measured and estimated states and the closed-loop system was shown to be globally asymptotically stable. Finally, it was also proven that the dynamics of the torsion angle remains bounded under the action of the controller; in particular it was shown that it is uniformly ultimately bounded. Simulation results have confirmed the effectiveness of the proposed approach.

APPENDIX

A. Dynamics of the Error Variable z

The error variable dynamics is given by

$$\begin{aligned}
\dot{z} &= \dot{\hat{\omega}}_g - \frac{\partial\alpha}{\partial\hat{\theta}_k}\dot{\hat{\theta}}_k - \frac{\partial\alpha}{\partial e_\omega}\dot{e}_\omega - \frac{\partial\alpha}{\partial\boldsymbol{\Omega}_d}\dot{\boldsymbol{\Omega}}_d \\
&= \left(\frac{K_d}{J_gN_g} + \frac{N_gK_d\left(\beta_1+\beta_2\right)}{J_rB_d} - \frac{2k_wN_gK_d}{J_rB_d}\left(e_\omega+\omega_d\right)\right)\hat{\theta}_k \\
&\quad + \left(\frac{B_d}{J_gN_g} - \frac{N_gK_d}{B_d}\right)\left(e_\omega+\omega_d\right) \\
&\quad + \left[\frac{K_d}{B_d} - \frac{1}{J_g}\left(\frac{B_d}{N_g^2}+B_g\right)\right]\left[z+\alpha\left(\hat{\theta}_k, e_\omega, \omega_d, \dot{\omega}_d\right)\right] \\
&\quad - \frac{N_g}{B_d}\left[\left(\frac{B_d^3}{N_g^3}\beta_1 + K_d^2\beta_2\right) + B_d + B_r\right]\dot{\omega}_d + \frac{N_gJ_r}{B_d}\ddot{\omega}_d \\
&\quad - \frac{N_g}{J_rB_d}\left[-2k_w\left(e_\omega+\omega_d\right) - \left(\frac{B_d^3}{N_g^3}\beta_1 + K_d^2\beta_2\right)\right] \\
&\quad \times \left[k_w\left(e_\omega+\omega_d\right)^2 - \left(B_d+B_r\right)\left(e_\omega+\omega_d\right)\right] \\
&\quad - \frac{1}{J_r}\left[-2k_w\left(e_\omega+\omega_d\right) - \left(\frac{B_d^3}{N_g^3}\beta_1 + K_d^2\beta_2\right)\right] \\
&\quad \times \left[z+\alpha\left(\hat{\theta}_k, e_\omega, \omega_d, \dot{\omega}_d\right)\right] \\
&\quad - \frac{2k_wN_gK_d}{J_rB_d}\left(e_\omega+\omega_d\right)\tilde{\theta}_k - \frac{N_gK_d\left(\frac{B_d^3}{N_g^3}\beta_1 + K_d^2\beta_2\right)}{J_rB_d}\tilde{\theta}_k \\
&\quad + \frac{2k_w}{J_r}\left(e_\omega+\omega_d\right)\tilde{\omega}_g + \frac{\left(\frac{B_d^3}{N_g^3}\beta_1 + K_d^2\beta_2\right)}{J_r}\tilde{\omega}_g - \frac{1}{J_g}T_g
\end{aligned} \tag{55}$$

REFERENCES

[1] K. Hammerum, "A fatigue approach to wind turbine control. masters thesis, technical university of denmark," Master's thesis, Aalborg University, 2006.

[2] H. Khalil, *Nonlinear Systems*, Third ed. Prentice Hall, 2002.

[3] M. Krstić, I. Kanellakopoulos, and P. Kokotović, *Nonlinear and Adaptive Control Design*, S. Haykin, Ed. John Wiley and Sons, 1995.

[4] Z. Lu and W. Lin, "Asymptotic tracking control of variable-speed wind turbines," *IFAC World Congress*, vol. 18th, 2011.

[5] U. Ozbay, E. Zergeroglu, and S. Sivrioglu, "Adaptive backstepping control of variable speed wind turbines," *International Journal of Control*, vol. 81:6, pp. 910–919, 2011.

[6] C. Sloth, T. Esbensen, M. Niss, J. Stoustrup, and P. Odgaard, "Robust lmi-based control of wind turbines with parametric uncertainties," *Proceedings of the 3rd IEEE multi-conference on systems and control. Saint Petersburg, Russia*, p. 77681., 2009.

[7] C. Sloth, T. Esbensen, and J. Stoustrup, "Robust and fault-tolerant linear parameter-varying control of wind turbines," *Mechatronics*, vol. 21, pp. 645–659, 2011.

[8] Y. Song and B. D. X. Bao., "Variable speed control of wind turbine using nonlinear and adaptive algorithms," *Journal of Wind Eng. & Industr. Aerodynamics*, vol. 85, 2000.